UNUSUAL AQUEOUS DEPOSITS WITHIN THE MARTIAN METEORITE NAKHLA. K. L. Thomas-Keprta[1], S. J. Clemett[1], N. Baskar[2], Z. Rahman[1], E. K. Gibson[3], S. J. Wentworth[1], D. S. McKay[3]; [1]Jacobs JETS, NASA/JSC, Houston, TX 77058 (kathie.thomas-keprta-1@nasa.gov); [2]Liberty High School, Frisco TX 75035; [3]ARES, NASA/JSC, Houston, TX 77058; [3]Deceased, formerly ARES, NASA/JSC, Houston, TX 77058.

We report the first identification of two unique, aqueously altered, foliated assemblages on interior fracture surfaces of the martian meteorite Nakhla. The assemblages are of demonstrably martian origin, and are consistent with formation from low temperature, CO_2-rich, aqueous brines with variable compositions. They appear as micron-thick layers overlying an augite-rich groundmass. Each demonstrates chemical and structural partitioning with sharply delineated interfaces with gradients in the nanometer range. Although appearing superficially similar to iddingsite alteration features that have been previously well documented in Nakhla [*e.g.*, 1-3 and references therein], they contain no phyllosilicates and represent a distinct and separate type of alteration feature. One of the assemblages is composed of two amorphous Si-rich layers separated by a vein composed of a mixture of amorphous phases interspersed with nanophase crystallites, primarily carbonate along with minor Fe-(oxy)hydroxides and salts. The other assemblage has a single amorphous Si-rich layer overlain by a vein composed principally of poor-crystalline nanophase Fe-(oxy)hydroxides.

Previous studies of mineral weathering in Nakhla have invoked saturation-precipitation models to explain their observations [*e.g.*, 1, 2]. We suggest these new alteration features provide evidence for a recently proposed reaction mechanism for silicate weathering which proceeds through a coupled interfacial dissolution-reprecipitation mechanism [4, 5].

Methods: The Nakhla samples used in this work were acquired from the British Museum of Natural History. Chips from Nakhla, split 14, were fractured under clean conditions using stainless steel tools. Fragments which revealed fresh interior fracture surfaces were selected and photo-documented prior to being sputter-coated with Pt (~1 nm); they are characterized using field emission scanning electron microscopy (FESEM) and energy dispersive X-ray spectroscopy (EDX). Regions of interest (ROIs) were identified and subsequently extracted by focused ion beam (FIB) microscopy and thinned to electron transparency for characterization by field emission scanning transmission electron microscopy (FESTEM) and EDX.

Results: Figure 1A shows the fresh fracture surface of a Nakhla grain, with the region enclosed by the red box denoting the ROI in which the new alteration features were observed. Figure 1B shows an enlargement of the ROI with its layers designated 1 through 4, with the yellow rectangle indicating the location from which the

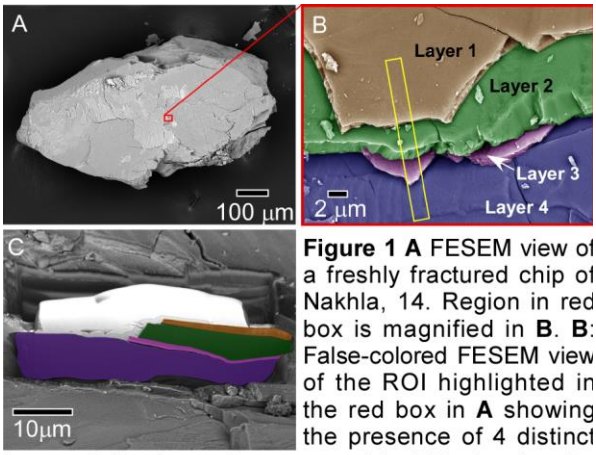

Figure 1 A FESEM view of a freshly fractured chip of Nakhla, 14. Region in red box is magnified in **B**. **B**: False-colored FESEM view of the ROI highlighted in the red box in **A** showing the presence of 4 distinct layers. **C** Region to be extracted by FIB showing the layers (false-colored, corresponding to those in **B**), prior to FIB milling.

transverse thin-section was extracted by FIB. Figure 1C shows the ion-milled thin-section just prior to extraction. The four distinct layers are vertically stacked with layers 2 & 4 composed of augite (in the same crystallographic orientation) and layers 1 & 3 representing alteration features. Composite high resolution FESTEM mosaics of layers 1 & 3 are shown in Fig. 2, and are ~6 × 1.5 µm^2 and ~10 × 1.0 µm^2 in size, respectively. Layer 1 contains three sublayers with the top and bottom being siliceous and composed of major Si, Mg, Fe, O, Cl with minor Na, Al, K, Ca and Mn. The siliceous sublayer in layer 3 has a similar composition to those in layer 1. All siliceous layers appear texturally amorphous, lacking detectable long range structural order. Occasionally embedded within the siliceous layers are fine-grain Fe-rich particles, typically <30 nm in size. It is noteworthy the interface between unaltered augite and the alteration layers 1 & 3 is extremely sharp and shows no evidence for differential etching and/or pitting.

The central vein in layer 1 is texturally and chemically complex; proceeding longitudinally from left to right, the Ca (and corresponding Mg & Mn) abundance is variable, as shown in Fig. 2. In general the Ca abundance in anti-correlated with the Fe, Si and Cl. The low C abundance, ~2 – 7 wt.%, indicates the presence of carbonate and non-carbonate phases. Figure 3 shows an expanded view of layer 1 along with accompanying EDX elements maps for Ca, Fe, Na, Mn, Cl & C illustrating the nanometer scale chemical gradients. Additionally overlapping spectra are shown for a Ca-rich and a Ca-poor region.

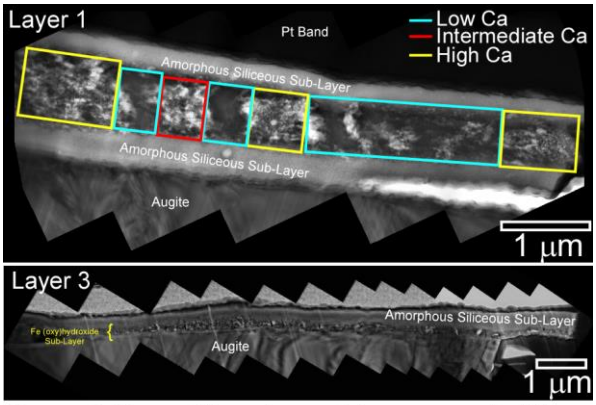

Figure 2. **Upper View**: Layer 1 is composed of three sub-layers, two of which are primarily amorphous silica. These siliceous layers sandwich a central layer composed of a mixture of carbonate and non-carbonate phases. This layer contains variable Ca-Fe-Mg-Mn (see also Fig. 3). **Lower View**: Layer 3 contains two layers, amorphous silica bordered by a layer composed primarily of fine-grain Fe-(oxy)hydroxide.

The Fe-rich sublayer in Layer 3 (see Figs. 2 & 4) is composed primarily of fine-grain, polycrystalline Fe-(oxy)hydroxides, with one phase identified as ferrihydrite. This sublayer also contains major O, Si, Mg, Mn, Na, Ca & C (~1.5 wt.%) with minor K & Ca.

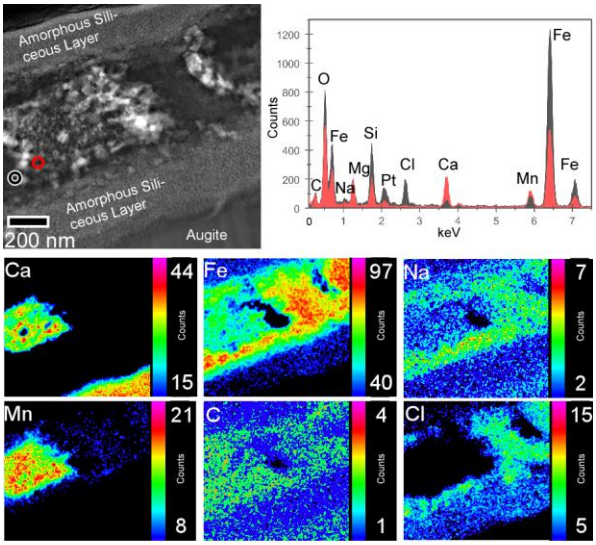

Figure 3. **Upper View, Left**: FESTEM view of a section of layer 1 showing three sublayers, two of which are primarily amorphous silica that border a center sub-layer. **Upper View, Right**: Overlapping EDX spectra of the regions highlighted by the circles in the Upper Left View. Spectra were taken for 250 s. and are ~100 nm apart. **Lower Views**: Element maps for Ca, Fe, Na, Mn, C & Cl show the extent of chemical variation within the middle sublayer of layer 1.

Discussion: The absence of any discernible phyllosilicates in these alteration assemblages differentiates them from the 'conventional' description as iddingsite. Instead we suggest formation, at least in part, through a

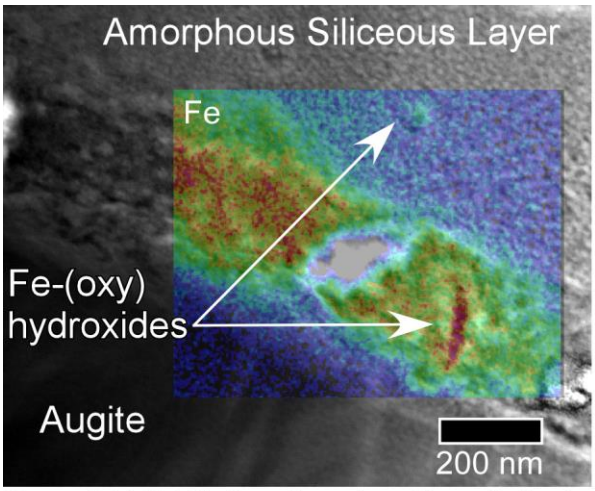

Figure 4. FESTEM view of a region of layer 3 showing the amorphous siliceous layer bordered by the Fe-rich layer. The overlying EDX element map for Fe highlights the locations of two Fe-bearing grains, one in the siliceous layer and one in the Fe-rich sublayer.

new model called coupled dissolution-reprecipitation, described in detail by Hellmann et al. [4, 5]. In this model, altered mineral surfaces are characterized by a distinct surface layer that is amorphous, less dense, and enriched in silica compared to the host mineral. The surface layers are characterized by sharp changes in cation concentrations that are spatially coincident with the amorphous-crystalline interface. Since the precipitated silica layer sequesters variable amounts of other cations released from the parent mineral, it acts as a sink for divalent metal cations. Interestingly, elevated CO_2 concentrations (in solution) results in the precipitation of amorphous silica layers containing cations overlain by carbonate precipitates. Hellmann et al. [4] speculate that higher water:mineral ratios (*i.e.*, undersaturated conditions) are needed for this model; when these ratios are too low (*i.e.*, fluids saturated in silica), the porous structure of the silica layers can become partially plugged with nano-sized carbonate or phyllosilicate crystallites and limit transport of aqueous reactants and products through the silica layers. We did not observe either carbonate or clay crystallites, but did find nanophase Fe oxy(hydroxides) heterogeneously embedded in silica layers, as shown in Fig. 4.

References: [1] Lee *et al*. (2015) *Geochim. Cosmochim. Acta* 154, 49-65. [2] Changela & Bridges (2011) *Meteorit. Planet. Sci*. 45, 1847-1867. [3] Treiman (2005) Chemie der Erde 65, 203-270. [4] Hellmann *et al*. (2013) *Procedia Earth & Planet. Sci*. 7: 346-349. [5] Hellmann *et al*. (2015) Nature Materials. DOI 10.10.1038/NMAT4172.

Acknowledgements: Funding provided by NSF/AAG and NASA/EW programs. We thank Michael Velbel for valuable discussions.